Journal of NeuroVirology, 11: 281–291, 2005
© 2005 Journal of NeuroVirology
ISSN: 1355-0284 print / 1538-2443 online
DOI: 10.1080/13550280590952835

Taylor & Francis
Taylor & Francis Group

Cocaine increases human immunodeficiency virus type 1 neuroinvasion through remodeling brain microvascular endothelial cells

Milan Fiala,[1] Amy J Eshleman,[2] John Cashman,[3] Justin Lin,[1] Albert S Lossinsky,[4] Vannina Suarez,[1] Wendy Yang,[1] Jun Zhang,[3] Waldemar Popik,[5] Elyse Singer,[6] Francesco Chiappelli,[7] Eva Carro,[8] Martin Weinand,[9] Marlys Witte,[9] and James Arthos[10]

[1]Department of Medicine, West Los Angeles VA Medical Center, Los Angeles, California, and UCLA School of Medicine, Los Angeles, California, USA; [2]Department of Pharmacology, VA Medical Center, Portland, Oregon, USA; [3]Human BioMolecular Research Institute, San Diego, California, USA; [4]Huntington Medical Research Institutes, Pasadena, California, USA; [5]Oncology Center, The Johns Hopkins University School of Medicine, Baltimore, Maryland, USA; [6]Department of Neurology, UCLA School of Medicine, Los Angeles, California, USA; [7]Department of Oral Biology and Medicine, UCLA School of Dentistry, Los Angeles, California, USA; [8]Laboratory of Neuroendocrinology, Cajal Institute, CSIC, Madrid, Spain; [9]Department of Surgery, University of Arizona, Tucson, Arizona, USA; and [10]Laboratory of Immunoregulation, National Institute of Allergy and Infectious Diseases, National Institutes of Health, Bethesda, Maryland, USA

Cocaine is a suspected cofactor in human immunodeficiency virus (HIV)-associated dementia but cocaine's effects are not clear. Herein the authors describe investigations of the mechanisms by which cocaine increases HIV-1 invasion through brain microvascular endothelial cells (BMVECs). Cocaine binds to a site on BMVECs, which is not a biogenic amine transporter, a binding site for estrogen, or a muscarinic receptor and for which benztropine and tamoxifen have the highest affinity. Cocaine treatment of BMVECs disrupts intercellular junctions and induces cell ruffling, which could account for their increased permeability and decreased electrical resistance. HIV-1 enters BMVECs by macropinocytosis and is transported to lysosomes and inactivated. In cocaine-treated BMVECs, the virus enters and persists in large cytoplasmic "lakes." Cocaine exposure of BMVECs up-regulates transcription of genes important in cytoskeleton organization, signal transduction, cell swelling, vesicular trafficking, and cell adhesion. The toxicity of cocaine for the blood-brain barrier may lead to increased virus neuroinvasion and neurovascular complications of cocaine abuse. *Journal of NeuroVirology* (2005) **11,** 281–291.

Keywords: cocaine; brain microvascular endothelial cells; HIV-1; HIV-1 macropinocytosis

Introduction

Cocaine abuse has been associated with neurological complications, including cerebral infarction or hemorrhage, brain aneurysms, transient ischemic attacks, migraines, seizures, vasculitis (Kokkinos and Levine, 1993), and human immunodeficiency virus (HIV)-1–associated dementia (HAD) (Bouwman *et al*, 1998) (Holman *et al*, 1992). HAD is a subcortical dementia (Price and Brew, 1988) characterized by deteriorating cognitive and motor functions and behavior, and its risk has been related to HIV-1 load in brain monocyte/macrophages (MMs) (Wiley *et al*, 1999) or the number of infected MM's (Glass *et al*, 1995). Early

Address correspondence to Milan Fiala, UCLA Oral Biology and Medicine, CHS 63-090, 10833 Le Conte, Los Angeles, CA 90095, USA. E-mail: Fiala@ucla.edu
This work was supported by National Institutes of Health grants DA10442, HL63639, and HK63065 to M.F., AI42557 and AI50461 to W.P., and HL48493 to M.W. The Manhattan HIV Brain Bank, New York, and the National Neurological AIDS Brain Bank at UCLA, Los Angeles, of the National NeuroAIDS Tissue Consortium provided the brain tissues. The AIDS Research and Reference Reagent Program, NIAID, National Institutes of Health, provided the listed antibodies. We appreciate discussions with P. Shapshak, University of Miami, regarding complications of cocaine abuse. Daniel Mcelligot, (VizX, GeneSifter Inc.) provided excellent technical support with the analysis of microarray data.
Received 6 December 2004; revised 1 February 2005; accepted 8 February 2005.

after HIV-1 infection, even before macrophage infiltration of the brain, HIV-1 (Resnick *et al*, 1988; Davis *et al*, 1992) and simian immunodeficiency virus (Sharma *et al*, 1992) invade the brain probably using the mechanisms of macropinocytosis and transcytosis through brain microvascular endothelial cells (BMVECs) (Liu *et al*, 2002). HIV-1 binds in BMVECs to GM1 ganglioside (Liu *et al*, 2002) and heparan sulfate proteoglycans (Bobardt *et al*, 2004). NeuroAIDS (acquired immunodeficiency syndrome) progression may be related to Trojan transport of HIV-1 in MMs and lymphocytes (Williams and Hickey, 2002). Epidemiological and neurovirological data support the role of cocaine in HAD (Goodkin *et al*, 1998), for which multiple mechanisms have been considered: synergistic neurotoxicity of cocaine with HIV-1 (Koutsilieri *et al*, 1997), potentiation of HIV-1 replication (Bagasra and Pomerantz, 1993), up-regulation of adhesion molecules and leukocyte transmigration (Gan *et al*, 1999), and increase in proinflammatory cytokines (Gan *et al*, 1998b) and HIV-1 permeability across BMVEC's (Zhang *et al*, 1998). Cocaine could increase virus neuroinvasion through BMVECs by direct effects and by paracrine effects of inflammatory cytokines (Zhang *et al*, 1998b). To clarify the cellular and molecular mechanisms of cocaine in BMVECs, we have examined cocaine's binding to endothelial cells, disruption of cell junctions, and remodeling microvascular and macrovascular endothelial cells. Using microarray analysis, we have identified cocaine-induced transcriptional alterations, which could be related to vascular and infectious complications of cocaine abuse, including augmented HIV-1 neuroinvasion.

Results

The cocaine-binding site on BMVECs is not a biogenic amine transporter, estrogenic binding site, or a muscarinic receptor

To investigate the binding of cocaine to BMVECs, we initially examined the presence of biogenic amine transporters. mRNAs for biogenic amine (norepinephrine and serotonin) transporters were detected in mouse brain endothelial cells (Wakayama *et al*, 2002). However, in intact adherent human BMVECs we found no specific uptake of [^{3}H]dopamine, [^{3}H]serotonin, or [^{3}H]norepinephrine by neurotransmitter uptake assays that are routinely used to measure uptake in cells transfected with neurotransmitter transporters and brain preparations. To characterize the pharmacology of the binding site for cocaine in BMVEC membranes, we used the aryl tropane analog [^{125}I]RTI-55 as a ligand. [^{125}I]RTI-55 is more stable than cocaine, due to the removal of the C-3 ester linkage, has a higher specific activity than [^{3}H]cocaine, and has been used extensively to examine the binding site for cocaine on biogenic amine transporters (Eshleman *et al*, 1999). Binding of [^{125}I]RTI-55 to BMVEC membranes showed saturable binding characteristic of a reversible protein interaction. The density (B_{max}) of [^{125}I]RTI-55 binding sites in the membranes was 2.45 ± 0.29 pmol/mg protein with an affinity (K_d) of 152 ± 45 nM. We examined an array of agents selective for various transporters and receptors as competitive ligands to characterize the pharmacology of [^{125}I]RTI-55 binding (Figure 1). Benztropine and tamoxifen had the highest affinities for this site (K_i values = 19.4 ± 4.2 and 21.4 ± 7 nM, respectively), and cocaine had cocaine had less potency (K_i = 6500 ± 1800 nM). The affinity of mazindol for this binding site (i.e., 41,000 ± 18,000 nM) was 1000-fold lower than its affinity for the dopamine transporter. In addition, the affinity of verapamil for the site (8700 ± 2400 nM) was 10-fold lower than its affinity for P-glycoprotein (Brust *et al*, 2000). The rank order of affinity was benztropine > tamoxifen > RTI-55 > GBR 12935 > bupropion > cocaine = verapamil > methamphetamine > mazindol > serotonin > dopamine (Table 1). Although tamoxifen had high affinity for the binding site, 17β-estradiol-glucuronide was not potent at inhibiting [^{125}I] RTI-55 binding. Thus, the pharmacology was not that of a traditional biogenic amine transporter or an estrogenic binding site. The correlation coefficient of K_i with the polar surface area (PSA) was insignificant (r = .07, P = .43), suggesting that capacity of compounds for passive transport through membranes was not the primary determinant of affinity at this site.

Because functional acetylcholine muscarinic receptor has previously been observed in BMVECs. (Elhusseiny *et al*, 1999) and the muscarinic receptor ligand benztropine was potent at the [^{125}I]RTI-55 binding site, we examined the presence of the

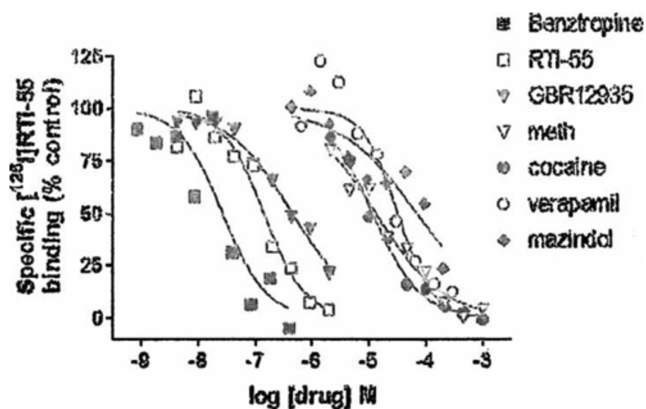

Figure 1 Inhibition of^{125} I-RTI binding to BMVECs by biogenic amines. Inhibition studies were conducted with ^{125}I-RTI (80 to 100 pM), BMVEC membranes, and the indicated concentrations of the inhibitors. For each compound, three or more independent competition experiments were conducted with duplicate determinations using nine concentrations. Data are from a representative experiment that was repeated three times with similar results. The average K_i values plus SEM are given in Table 1. Meth = methamphetamine.

Table 1 Pharmacology of the cocaine-binding site on brain endothelial cell membranes: Inhibition of [^{125}I]RTI-55 binding by biogenic amines and other ligands[a]

Drug	*K_i (±SEM) (nM)*	*Hill coefficient[b] (±SEM)*
Benztropine	19.4 ± 4.2	0.85 ± 0.14
Tamoxifen	21.4 ± 7.0	1.24 ± 0.17
RTI-55	110 ± 17	1.45 ± 0.29
GBR 12935	370 ± 110	0.69 ± 0.09
Bupropion	3000 ± 950	1.03 ± 0.16
Cocaine	6500 ± 1800	0.92 ± 0.06
Verapamil	8700 ± 2400	0.94 ± 0.12
Methamphetamine	11600 ± 3100	0.93 ± 0.10
17β-Estradiol -glucuronide	>10 μM	
Mazindol	41,000 ± 18,000	0.73 ± 0.06
5-Hydroxytryptamine	6.0 ± 1.1 mM	0.90 ± 0.15
Dopamine	19.7 ± 1.9 mM	1.50 ± 0.26

[a]Each assay was replicated three to five times. GraphPAD Prism was used to analyze the data. IC_{50} values were converted to K_i values using the Cheng-Prusoff equation, as described in Materials and Methods.
[b]A Hill coefficient near 1 suggests competitive interactions of the test compound with the radioligand, whereas a Hill coefficient other than 1 suggests complex drug interactions at binding sites.

muscarinic receptor. We amplified full-length muscarinic 1 receptor (M1) mRNA from total BMVEC RNA by reverse transcriptase–polymerase chain reaction (RT-PCR) with M1-specific primers. The DNA sequence observed was identical to the M1 receptor (i.e., Gene Bank accession no. NT-033903) with the exception that nucleotides GA at positions 516 and 517 were present as AG. With evidence that the M1 receptor was present in BMVECs, we tested an array of compounds with high potency at one or more of the muscarinic receptor subtypes for affinity at the binding site. The nonselective muscarinic antagonist 4-DAMP had the highest affinity (430 ± 270 nM), an $IC_{50} \sim 400$ times higher than its K_i; at muscarinic receptors (Caulfield and Birdsall, 1998). Neither the antagonists chlorpromazine (700 ± 200 nM), atropine (sulfate or free base, 2760 ± 710 or 8000 ± 2100 nM), AFDX 116 (>100 μM), and pirenzepine (>1 mM) nor the agonists oxotremorine (>1 mM) and pilocarpine (>1 mM) had affinity for the binding site. The muscarinic antagonist [^{3}H]QNB was displaced by micromolar or millimolar concentrations of the muscarinic ligands. Thus, the lack of potency of muscarinic ligands for the [^{125}I]RTI-55 binding site was not consistent with that of a muscarinic receptor.

Cocaine treatment of BMVECs enhanced virus invasion through BMVECs (Zhang *et al*, 1998). To examine relevant mechanisms, we performed microscopic and functional studies of micro- and macrovascular endothelial cells using cocaine concentrations in 10 and 1 μM and lower concentrations (death from cocaine overdose occurs at 1 to 5 μM cocaine concentrations in the brain; personal communication, L. Hearn, Asst. Medical Examiner, Miami).

Cocaine induces interendothelial gaps and decreases transendothelial electrical resistance (TEER)

Cocaine (10^{-5} to 10^{-8} M) treatment of BMVECs and coronary artery endothelial cells (CAECs) produced interendothelial gaps (Figure 2), whereas human aortic endothelial cells (HAECs), human pulmonary artery endothelial cells (HPAECs), and human umbilical vein endothelial cells (HUVECs) were not affected. Cocaines effects were noted only with BMVECs and CAECs at a low *in vitro* passage (1 to 5), whereas the cells seemed resistant at higher passages. The disruption was noted after 30 min and became maximal after 1 h and was visible by immunofluorescence after staining with phalloidin and by phase-contrast microscopy. Pretreatment with tyrosine kinase inhibitor genistein (1.5 to 15 μg/ml) blocked the effect of cocaine.

To observe cocaine's effects on endothelial barrier function in real time, we measured TEER over 24 h. In the concentration range 10^{-4} to 10^{-8} M, cocaine reduced TEER during the 24-h observation period below that of untreated cells, whereas 10^{-9} M cocaine increased TEER (Figure 3).

To examine cocaine's ultrastructural effects, we performed electron and confocal microscopy.

Cocaine induces cytoplasmic ruffling of BMVECs and CAECs

In CAECs and BMVECs treated with 1 or 10 μM cocaine, scanning electron microscopic (SEM) examination revealed intense ruffle formation in addition to the disruption of interendothelial junctions corresponding to those seen by fluorescence microscopy (Figure 4).

Cocaine disrupts actin cytoskeleton and enhances HIV-1 entry into large "lakes"

HIV-1-GFP enters BMVECs (Liu *et al*, 2002) and CAECs (Gujuluva *et al*, 2001) by macropinocytosis, is transported to lysosomes, and lysed. We examined by confocal microscopy the entry of HIV-1-Vpr-GFP in parallel cultures of BMVECs, which were kept either in control medium or in medium supplemented with 10^{-5} M cocaine. In the cells kept in control medium, HIV-1-Vpr-GFP entered the cell through a surface crater 30 min post infection (p.i.), travelled along actin filaments at 3 and 6 h (note yellow colocalization of green fluorescent protein [GFP] with Texas Red–actin), and arrived into perinuclear vacuoles, which fused with lysosomes by 18 h p.i. (Figure 5b). In cocaine-treated cells, this pattern was completely disrupted: at 1.5 h p.i., HIV-1-Vpr-GFP invaded large cytoplasmic "lakes" and persisted there until 18 h p.i. In cocaine-treated cells invaded by the virus, the actin cytoskeleton appeared disrupted (Figure 5a).

Cocaine alters transcriptional program in BMVECs

Two replicate experiments were performed with BMVECs treated by 10^{-5} M cocaine for 6 or 24 h. RNA

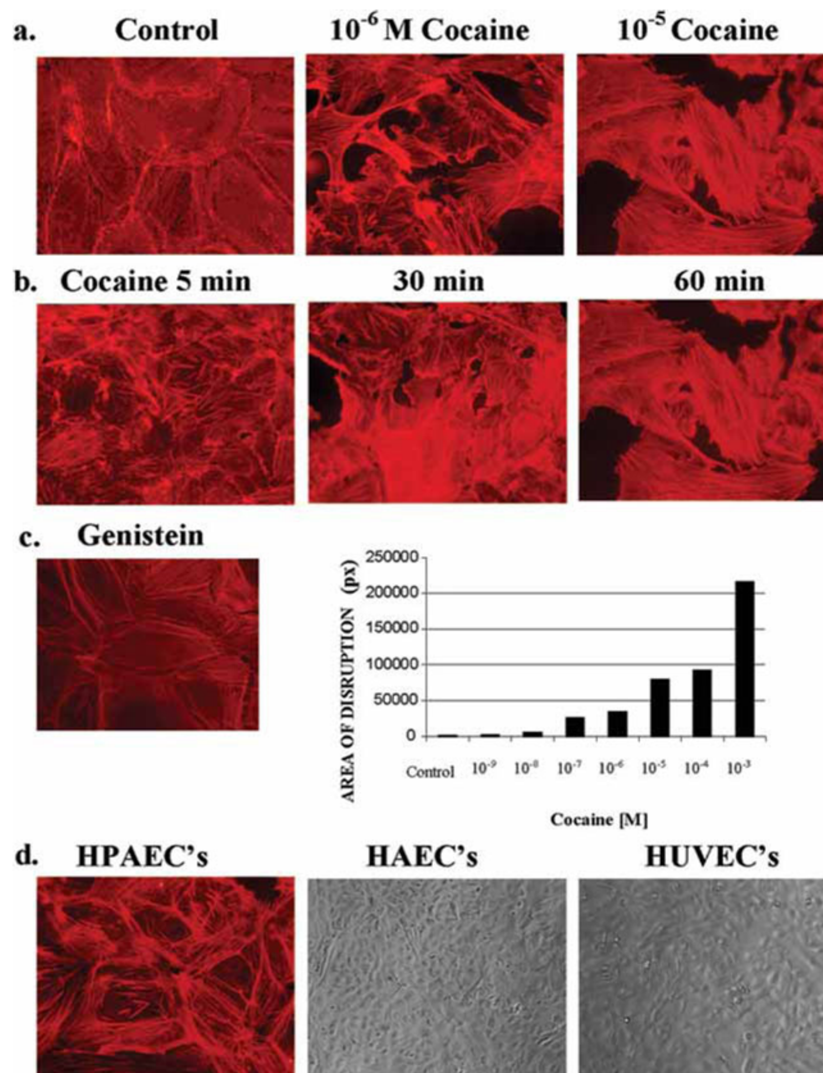

Figure 2 Cocaine induces interendothelial gaps in BMVECs. Confluent BMVECs on coverslips were treated with the indicated concentrations of cocaine or an inhibitor. **a,** Dose response: cocaine treatment for 60 min; **b,** time course: cocaine treatment for 5, 30, or 60 min; **c,** inhibition study: pretreatment with genistein (10 μg/ml) for 60 min followed by treatment with 10^{-6} M cocaine for 60 min; **d,** lack of effect on other endothelial cells: 60-min 10^{-6} M cocaine treatment of macrovascular endothelial cells. (Phalloidin–Texas Red immunofluorescence with 40× objective.)

was extracted and transcribed, and fragmented cRNA hybridized to Affymetrix Microarrays. The signal values were analyzed and significant differentially expressed genes were subjected to Partitioning Around Medioids (PAM) clustering:

Cluster 1: Genes down-regulated at 6 h;
Cluster 2: Genes up-regulated at 6 h;
Cluster 3: Genes up-regulated at 24 h;
Cluster 4: Genes down-regulated at 24 h;
Cluster 5: Genes up-regulated at 6 and 24 h;
Cluster 6: Genes down-regulated at 6 and 24 h.

We analyzed significantly overrepresented genes in each cluster (Table 2). Transcriptional alterations involved cell metabolism, function, and structure with specific impact on endothelial cells and macrophages. In cluster 1, the down-regulation of fibroblast growth factor receptor 1, DNA (cytosine-5)-methyltransferase 3α, potassium voltage-gated channel, and transportin 2 could affect endothelial cell growth and integrity. In cluster 2, up-regulated adrenergic α 1A receptor, purinergic receptor P2Y, and dopamine receptor D2 could alter calcium and cAMP signaling resulting in alteration of endothelial cell function. In cluster 3 the up-regulated genes, colony-stimulating factor 2 receptor and macrophage scavenger receptor 1, have role in macrophage growth and endocytic function. The up-regulated mitochondrial uncoupling protein might increase thermogenesis. In

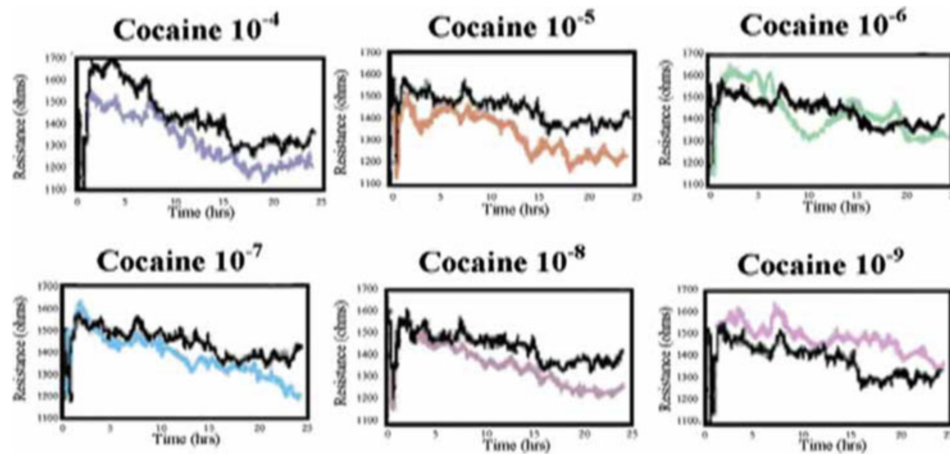

Figure 3 Cocaine induces decrease in transendothelial electrical resistance. Confluent BMVEC monolayers were prepared in 8-well chamber slides (Applied Biophysics), changed to medium with the indicated concentration of cocaine, and incubated in the ECIS apparatus with TEER monitoring over a 24-h period.

cluster 4, the down-regulated genes include (a) activin A receptor, type IB. Activins are transforming growth factor-β (TGF-β) superfamily growth and differentiation factors, which signal through receptor serine kinases and their decreased signaling might lead to greater endothelial cell proliferation; (b) aryl hydrocarbon receptor, which has a role in induction of enzymes of xenobiotic metabolism;

Table 2 Transcriptional alterations by cocaine treatment of BMVECs for 6 or 24 h

		Change at	
Culster no.	*Gene*	*6 h*	*24 h*
1	Fibroblast growth factor receptor 1	−1.64	
	DNA (cytosine-5-)methytransferase 3 alpha	−2.03	
	Postassium Volltage-gated channel, shaker-related subfamily, β member 2	−2.04	
	Transportin 2 (importin 3,karyopherin β 2b)	−1.82	
2	Adrenegic, α-1A, receptor	1.80	
	Purinergic receptor P2Y, G-protein coupled, 1	1.69	
	Dopamina receptor D2	1.49	
3	Colony-stimulating factor 2 receptor, alpha, low-affinity (granulocyte-macrophage)		1.68
	Macrophage scavenger receptor 1		1.67
	Uncoupling protein 1 (mitochondrial, proton carrier)		1.53
4	Activin A receptor, type IB		−1.63
	aryl hydrocarbon receptor nuclear translocator		−1.53
	Neuropeptide Y receptor Y2		−1.40
	Thyroid-stimulating hormone receptor		−1.28
	Chemokine (C-C motif) ligand 24		1.69
	ets variant gene 4 (E1A enhancer binding protein, E1AF)		−1.67
	Stabilin 2		−1.57
	ADP-ribosylation factor guanine nucleotide-exchange factor 2 (brefeldin A-inhibited)		−1.70
	Endothelial cell growth factor 1 (platelet-derived)		−1.63
	Growth differentiantion factor 10		−1.99
5	Solute carrier family 13 (sodium-dependent dicarboxylate transporter), member 3	2.28	1.62
	Chloride channel, calcium activated, family member 1	1.63	1.91
	Chloride channel, calcium activated, family member 2	1.39	1.29
	CD36 antigen (collagen type I receptor)	1.70	1.4
	Cytochrome P450, family 21, subfamily A, polypeptide 2	1.29	1.36
	Flotillin 1	2.36	1.68
6	Ropporin, rhophilin associated protein I	−1.5	−1.66
	LIM domain kinase I	−1.36	−1.25
	Protein tyrosine phosphatase, receptor type	−1.35	−1.22
	Proteoglycan 4, (megakaryocyte stimulating factor)	−1.31	−1.31
	Serine (or cysteine) proteinase inhibitor, clade A, member 1	−1.28	−1.41
	Natriuretic peptide receptor A/guanylate cyclase A	−1.51	−1.48
	CD1E antigen, e polypeptide	−1.65	−1.67
	Chemokine (C-X3-C motif) receptor 1	−1.3	−1.47

a. SEM

Control

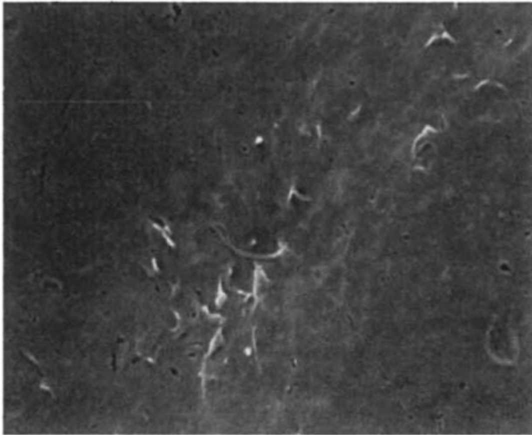

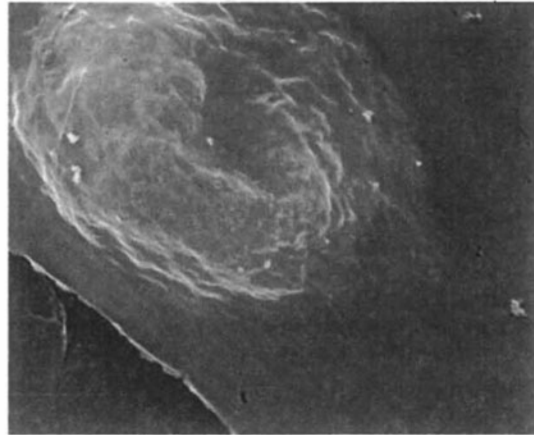

Cocaine 10^{-6} M

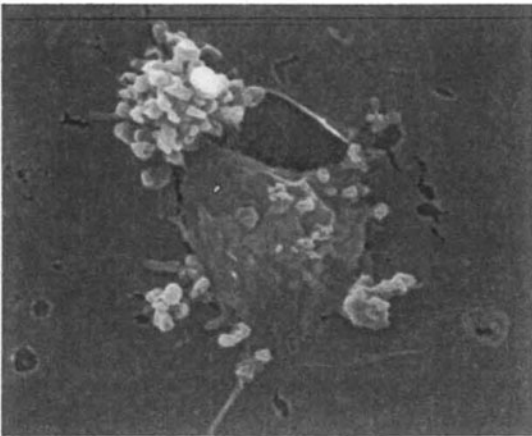

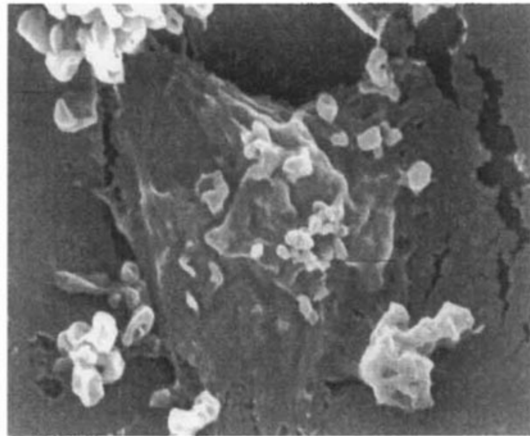

Cocaine 10^{-5} M

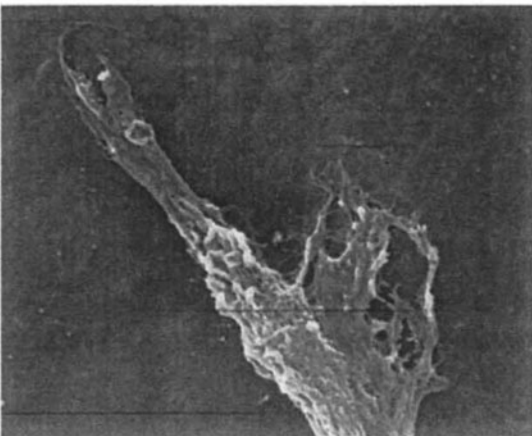

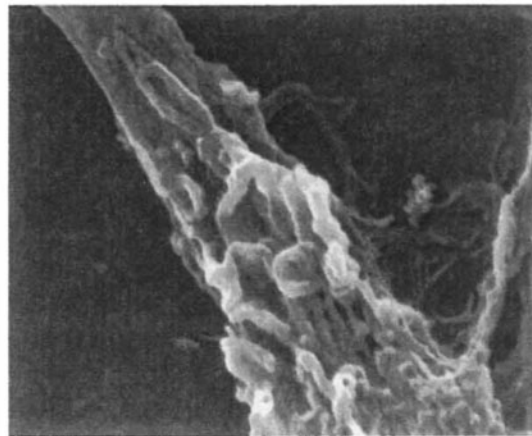

Figure 4 Cocaine treatment induces gaps and ruffling of BMVECs. Confluent BMVEC monolayers on plastic coverslips were exposed to medium with the indicated concentration of cocaine for 3 h, fixed, and processed for scanning electron microscopy.

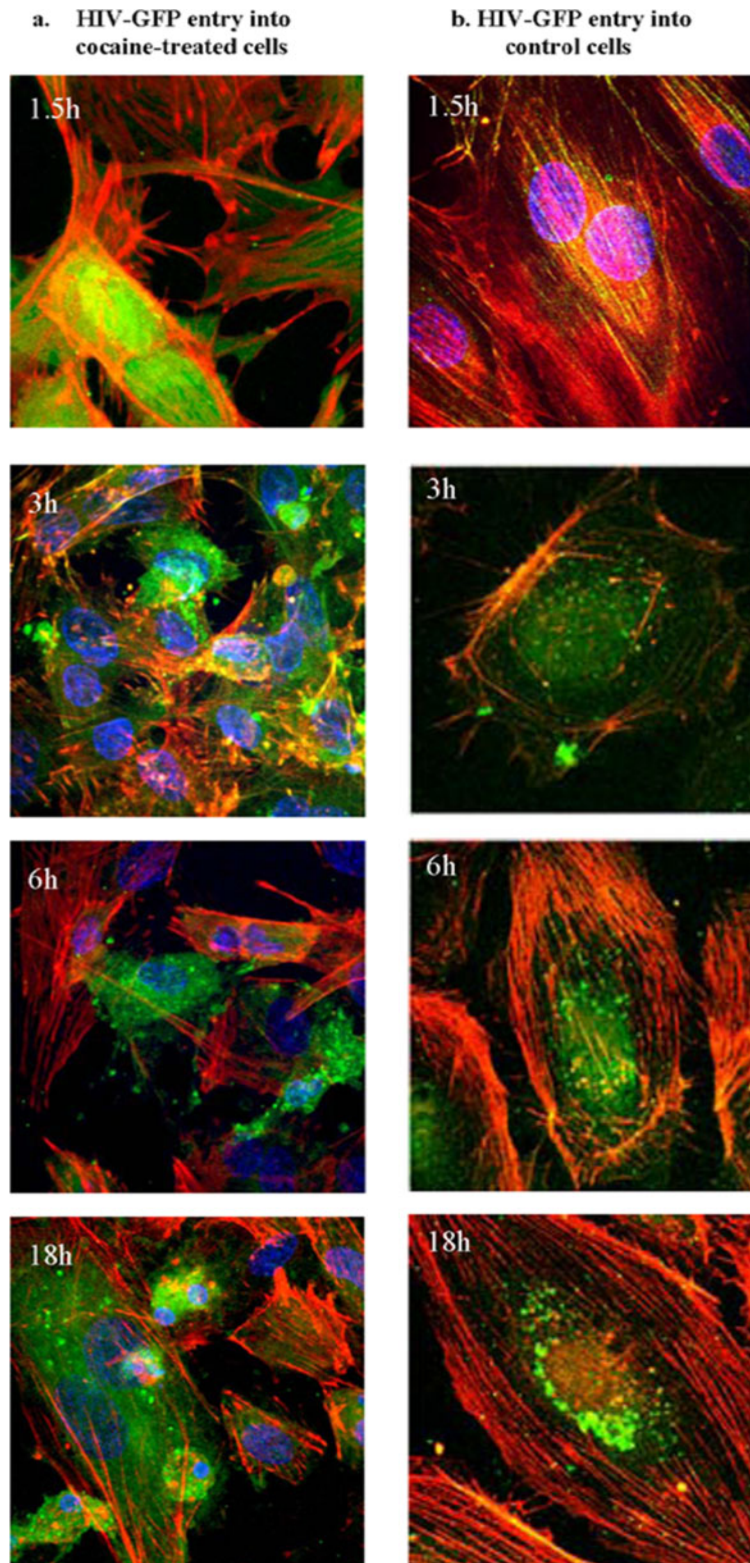

Figure 5 HIV-1 GFP entry is enhanced in BMVECs treated by cocaine. **a,** Medium with cocaine (10^{-5} M); **b,** control medium. Confluent monolayers of BMVECs on glass coverslips coated with gelatin were infected with HIV-1 GFP (10^8 RNA copies) in medium with 1 μM cocaine or control medium for the indicated time when they were fixed, stained by phalloidin–Texas Red, and examined by confocal microscopy (HIV-1 GFP is green, phalloidin–Texas Red is red, overlap is yellow; confocal microscopy, 100×).

(c) neuropeptide Y receptor Y2, which has a role in feeding and locomotor behavior; (d) thyroid-stimulating hormone receptor, which has a role in positive regulation of cell proliferation; (e) stabilin with a role in cell adhesion; (f) ADP-ribosylation factor (ARF) guanine nucleotide-exchange factor 2 with a role in activation of ARF's important in intracellular vesicular trafficking; (g) endothelial cell growth factor 1 (platelet-derived), which promotes angiogenesis and growth of endothelial cells. In cluster 5 up-regulated genes for chloride channel family have a role in sodium and chloride transport and could cause cell swelling. In addition, genes for CD36 antigen (collagen type I receptor), cytochrome P450 (family 21, subfamily A, polypeptide 2), and flotillin were up-regulated. In cluster 6 down-regulated genes with a role in cell-cell adhesion (rhophillin associated protein 1), protein-protein interactions (LIM domain kinase 1), acute response (protein tyrosine phosphatase, alpha-1-antitrypsin), immune response (CD1E antigen, chemokine C-X3-C receptor 1), and cardiovascular function (natriuretic peptide receptor A/guanylated cyclase A) were observed.

Discussion

Herein we report data that show (a) cocaine has a binding site on BMVECs; (b) cocaine disrupts endothelial cell junctions and induces cytoplasmic remodeling in BMVECs and CAEC's; (c) cocaine alters the transcriptional program of BMVECs; (d) cocaine alters the mode of HIV-1 entry and persistence in BMVECs. These effects of cocaine could promote HAD by increasing HIV neuroinvasion. In a previous study an HIV-1–positive patient with a history of cocaine abuse developed rapidly progressive dementia (Nath *et al*, 2001). These investigators also presented evidence based on animal studies that stimulant drugs have synergistic neurotoxicities with HIV-1. (Nath *et al*, 2002). In addition to direct effects on endothelial cells, other mechanisms of cocaine may be important in enhancement of neuropathogenesis. For example, cocaine alters the cytokine secretion profile to proinflammatory Th1-type, which may potentiate inflammatory activation of endothelial cells, induce adhesion molecules, and promote Trojan transport (Gan *et al*, 1998a; Gan *et al*, 1999). Cocaine induces secretion of C-X-C and C-C chemokines and tumor necrosis factor-αgy monocytes (Zhang *et al*, 1998).

Although we have amplified muscarinic M1 receptor mRNA in BMVECs and functional acetylcholine muscarinic receptor expression in human brain microvessels was previously observed (Elhusseiny *et al*, 1999), the binding site for cocaine on BMVECs and CAECs does not appear to be either a muscarinic receptor or a biogenic amine transporter. Recently, Deng *et al* (2002) showed that cocaine binds covalently to lysine residues of proteins. The time course for covalent bond formation was such that there was no binding at 5 min and measurable binding after 3 days. The cocaine analog that we used to label the cocaine binding site in BMVECs, [^{125}I]RTI-55, reached equilibrium binding by 50 min (data not shown), and cocaine was able to compete with [^{125}I]RTI-55 for this binding site at this time. This relatively rapid association rate strongly suggests that the binding is a drug/binding site interaction, and not a slow covalent bond formation. The data fit traditional saturable, reversible receptor binding isotherms. Second, analysis of the data to provide IC_{50} or K_i value gives no suggestion that the data are askew or not conforming to typical reversible binding data. Third, and in data not presented, we examined another series of tropanes and saw some dramatic differences associated with the stereochemistry of the ligand. If the receptor was acting normally, one would expect the stereoselectivity observed. If the receptor was acting as a simple acylation nucleophile, it would not pay any attention to stereochemical centers but rather act uniformly and treat all cocaine-like esters uniformly. That this is not observed suggests that the receptor is acting like other receptors: in a stereoselective and reversible fashion.

Cocaine's effects on endothelial cells resemble those of the well known edemagenic factor, thrombin, which produces endothelial gaps and disturbs the function of the endothelial barrier primarily via increase in actomyosin-based contraction (Borbiev *et al*, 2003). Signaling by thrombin has been recently recognized to involve multiple signaling pathways through activation of heterotrimeric G proteins, which inactivate adenylate cyclase by G_i-linked receptor or activate phospholipase C by G_q-dependent action (Bogatcheva *et al*, 2002). Although our investigation with cocaine has been difficult due to the restricted susceptibility of BMVECs to cocaine in early passage, we have shown that the tyrosine kinase inhibitor genistein inhibits cocaine-induced gap formation. Our preliminary data suggest that in BMVECs cocaine rapidly stimulates phosphorylation of extracellular signal-regulated kinases 1 and 2 (ERK1/2) (data not shown).

Cocaine treatment of BMVECs altered the transcriptional program in a complex fashion, with the net result leading to decreased cell adhesion, cell swelling, and impairment of signaling necessary for endothelial function. These changes involve ion channels, receptors mediating intracellular signaling, vesicular trafficking, cytoskeletal organization, angiogenesis, and specific cardiovascular function, which together would be expected to alter the function of BMVECs and CAECs. In conclusion, cocaine binds to a new site on BMVECs, remodels these cells, and increases their HIV-1 intracellular trafficking and invasion. Cocaine produces these effects by complex alteration of gene transcription.

Materials and methods

Reagents
Cocaine (free from endotoxin according to the Limulus lysate assay) (Research Triangle Institute, North Carolina); [^{125}I]RTI-55, [^{3}H]dopamine (46 Ci/mmol), [^{3}H]serotonin (28 Ci/mmol), and [^{3}H]norepinephrine (49 Ci/mmol) (NEN Life Science Products, Bostonm Massachusetts); wortmannin, herbimycin, genistein, staurosporine, U0126 (Calbiochem, San Diego, California); fluorescein isothiocyanate (FTIC)-conjugated phalloidin, antifade mounting medium, and Fura2/AM (Molecular Probes, Eugene, Oregon); thrombin, cyclodextrin, Limulus lysate endotoxin assay kit, 17β-estradiol-glucuronide, tamoxifen, dopamine, 2β-carbomethoxy-3β -(4-fluorophenyl)-tropane (CFT), 1-[2-diphenylmethoxy]ethyl-4-(3-phenylpropyl)-piperazine (GBR-12935) (Sigma, St. Louis, Missouri); gelatin (BD Diagnostic Systems, Sparks, Maryland).

Antibodies
Factor VIII (anti-von Willebrand factor) (DAKO, Carpinteria, California); anti-ZO-1 (Zymed, South San Francisco, California); anti-phospho-ERK1/2, anti-phospho-*cJun* N-terminal kinase (JNK) and anti-phospho-p38 mitogen activated protein kinase (Cell Signaling Technology, Beverly, Massachusetts).

Cell culture
BMVECs and CAECs were prepared and propagated as previously described. Briefly, BMVECs were isolated from temporal lobe tissues removed during epilepsy-related surgical procedures (Liu *et al*, 2002). Cocaine's effects have been demonstrated in at least four different BMVEC strains but only in early passages. CAECs were purchased from Clonetics (Walkersville, MD) (Gujuluva *et al*, 2001). Human macrovascular endothelial cells, pulmonary artery endothelial cells (HPAECs), HAECs, and HUVECs were obtained from Cascade Biologics (Portland, OR). Immortalized bovine BMVECs (Stins *et al*, 1997), named BMVEC-2, were provided by K-S Kim, Johns Hopkins University.

HIV-1$_{NL4-3}$-Vpr-GFP invasion and trafficking in BMVECs
HIV-1$_{NL4-3}$ incorporating Vpr-green fluorescent protein (GFP) (HIV-1 $_{NL4-3}$-Vpr-GFP) was prepared and applied to BMVECs as previously described (Liu *et al*, 2002). To visualize virus entry, the cells were fixed with 3% paraformaldehyde in phosphate-buffered saline (PBS), treated with PBS–1% bovine serum albumin (BSA), permeabilized with 0.1% Triton, washed with PBS, and stained with phalloidin–Texas Red (Sigma) and 4,6-Diamidino-2-phenylindole (DAPI). The preparations were examined using a Zeiss LSM 310 confocal microscope.

[^{3}H]Neurotransmitter uptake in, and [^{125}I]RTI-55 binding to, BMVEC-2 cells
[^{3}H]Neurotransmitter uptake was conducted as described with conditions optimized for BMVEC-2 cells in 6-well plates. Uptake was conducted with 20 nM [^{3}H]dopamine, [^{3}H]norepinephrine, or [^{3}H]serotonin for 20 min at 37°C using 5 μM mazindol or imipramine (for [^{3}H]serotonin) to define nonspecific uptake. Acid-soluble radioactivity was measured using a Beckman LS3800 counter.

[^{125}I] RTI-55 binding to BMVEC-2 cells
[^{125}I]RTI-55 binding was conducted as described (Eshleman *et al*, 1999). Cell membranes for cocaine binding studies, which were prepared from BMVECs, CAECs, or BMVEC-2s (the latter were used in experiments which required large amount of membranes), produced comparable results. The cells were grown to 90% confluence in 150-mm dishes. After washing the cells with calcium- and magnesium-free PBS, 10 ml of lysis buffer (2 mM HEPES with 1 mM EDTA) was added. Following lysis and centrifugation (30,000 × *g* for 20 min), the pellet was resuspended in 2.5 ml of sucrose (0.32 M) using a Polytron at setting 7 for 10 s. Each assay tube contained 60 to 100 μg of protein, 25 μl of drug or buffer, 80 to 100 pM [^{125}I]RTI-55, and buffer for a final volume of 250 μl. The time course of [^{125}I] RTI-55 binding to the cell membranes indicated that equilibrium was approached by 60 min (data not shown), thus all subsequent assays were conducted for 90 min. Nonspecific binding was defined using 1 mM cocaine. Using 60 to 100 μg of protein, specific binding was 500 to 800 counts per minute [CPM] and nonspecific binding was 80 to 120 CPM. Binding was terminated by filtration over Whatman GF/C filters using a Tomtec 96-well harvester. Filters were presoaked in 0.05% polyethylenimine to eliminate displaceable binding to the filters. Filters were washed for 6 s with ice-cold saline. Radioactivity on filters was determined using a Wallac betaplate reader. Data was analyzed using GraphPad Prism, with IC_{50} values converted to K_i values with the Cheng-Prusoff equation $\{K_i = IC_{50}/(1 + [L^*]/K_d^*)\}$, where L^* and K_d^* are the concentration and the affinity constant (152 nM), respectively, of the radioligand [^{125}I]RTI-55. To determine K_d and B_{max} values for RTI-55, competition experiments with unlabeled RTI-55 (10 nM to 5 μM) were conducted, and the data converted to saturation data by calculating the decrease in specific activity of [^{125}I]RTI-55. The K_d is the concentration of RTI-55 that is necessary to reach 50% of B_{max} in the saturation isotherm. For pharmacological characterization of the binding site, three or more independent competition experiments were conducted with duplicate determinations using nine concentrations. Molecular PSA is a descriptor that has a high correlation with passive molecular transport through intestinal and blood-brain barrier (BBB) membranes. PSA was calculated for the compounds

listed in Table 1 by the topological PSA method described previously (Ertl *et al*, 2000).

RT-PCR analysis of muscarinic receptor M1 gene transcription
Total RNA was prepared from primary BMVECs with Trizol reagent (Invitrogen, Carlsbad, California). The reverse transcription was performed with superscript II (Invitrogen). The muscarinic receptor (M1) gene was amplified using M1 specific PCR primers (5′ ATGAACACTTCAGCCCCACC and 5′ TCAGCATTG GCGGGAGGGAGT). The PCR reaction consisted of the following steps: 94°C for 2 min, followed by 35 cycles of 94°C for 30 s, 57°C for 30 s, 72°C extension for 1 min, and a final extension of 72°C for 5 min. The resulting PCR products were sequenced from both directions.

Immunofluorescence microscopy
Endothelial cells were grown to confluency on 1% gelatin-coated chamber slides. Cells were fixed with 4% paraformaldehyde, treated with 1% BSA for 30 min, and 0.1% Triton X-100 for 5 to 10 min before staining using primary antibodies to cell antigens and appropriate ALEXA-488 or Texas Red conjugated secondary antibodies, or phalloidin-FITC (1:40 in PBS) for 10 min at room temperature. Preparations were examined using BX60 Olympus microscope and photographed using DP11 Olympus camera.

Scanning electron microscopy (SEM)
After osmication and dehydration, the inserts or plastic coverslips with cell culture were dried with hexamethyldisalisane (Lossinsky and Shivers, 2003), attached to aluminum SEM stubs using double sticky carbon tape, then coated with gold and palladium and scanned on a FEI ESEM XL30 SEM.

Transendothelial electrical resistance (TEER)
BMVECs were cultivated in a humidified CO_2 incubator at 37°C in EGM-2-MV Bullet Kit medium (300 μl per well) in the 8W10E array comprising 8 separate wells on a glass slide with 10 microelectrodes per well connected to an electrical cell-substrate impedance-sensing system (Applied Biophysics, Troy, NY). Resistance was measured daily until approximately 1500-Ohm $\cdot$ cm^2 resistance was reached when the cells reached confluency (Garcia *et al*, 2000). After the drug had been added, the resistance was measured continuously for 24 h. Time-dependent average TEER values from each well were normalized as the ratio of measured resistance to baseline resistance.

Microarray procedure and data analysis
Total RNA from 3 million cells was extracted using the RNeasy Mini Protocol (Qiagen, Valencia, California) and 15 μg of RNA was used for microarray analysis. First- and second-strand DNA synthesis reactions were performed using the Superscript Choice system (Invitrogen) followed by *in vitro* transcription (Enzo Diagnostics). Fifteen microgram of fragmented cRNA was hybridized to Affymetrix U133 arrays A and B (Affymetrix, Santa Clara, California) by the procedure suggested by the manufacturer. The arrays were scanned by GeneArray Scanner (Hewlett Packard) and signal values obtained by Microarray Analysis Suite 5 Software were loaded. For analysis three groups with two replicate each were created. Each dataset was normalized to the mean signal value for the set. Analysis of variance (ANOVA) was performed on the three groups. Genes with $P < .05$ and a fold change of at least 1.5 in either the 6- or 24-h group relative to the control were selected. This filtering produced a list of 580 significantly differentially expressed genes. This group of genes was then subjected to PAM clustering (VizX; GeneSifter). Six clusters were created. Analysis of the clusters using silhouettes validated this selection. Three of these clusters showed up-regulation and three down-regulation. The genes in each cluster were analyzed using a *z*-score report for the biological process ontologies associated with the genes in the cluster. Ontologies with a *z*-score of >2 were considered to be significantly overrepresented in the cluster.

References

Bagasra O, Pomerantz RJ (1993). Human immunodeficiency virus type 1 replication in peripheral blood mononuclear cells in the presence of cocaine. *J Infect Dis* **168:** 1157–1164.

Bobardt MD, Salmon P, Wang L, Esko JD, Gabuzda D, Fiala M, Trono D, Van der Schueren B, David G, Gallay PA (2004). Contribution of proteoglycans to human immunodeficiency virus type 1 brain invasion. *J Virol* **78:** 6567–6584.

Bogatcheva NV, Garcia JG, Verin AD (2002). Molecular mechanisms of thrombin-induced endothelial cell permeability. *Biochemistry (Mosc)* **67:** 75–84.

Borbiev T, Garcia J, Verin AD (2003). Role of phosphorylation of myosin- and actin-binding proteins in thrombin-induced permeability of endothelial cells. *Russian J Bioorg Chem* **29:** 464–470.

Bouwman FH, Skolasky RL, Hes D, Selnes OA, Glass JD, Nance-Sproson TE, Royal W, Dal Pan GJ, McArthur JC (1998). Variable progression of HIV-associated dementia. *Neurology* **50:** 1814–1820.

Brust P, Friedrich A, Krizbai IA, Bergmann R, Roux F, Ganapathy V, Johannsen B (2000). Functional expression of the serotonin transporter in immortalized rat brain microvessel endothelial cells. *J Neurochem* **74:** 1241–1248.

Caulfield MP, Birdsall NJ (1998). International Union of Pharmacology. XVII. Classification of muscarinic acetylcholine receptors. *Pharmacol Rev* **50:** 279–290.

Davis LE, Hjelle BL, Miller VE, Palmer DL, Llewellyn AL, Merlin TL, Young SA, Mills RG, Wachsman W, Wiley CA (1992). Early viral brain invasion in iatrogenic human immunodeficiency virus infection. *Neurology* **42:** 1736–1739.

Deng SX, Bharat N, Fischman MC, Landry DW (2002). Covalent modification of proteins by cocaine. *Proc Natl Acad Sci U S A* **99:** 3412–3416.

Elhusseiny A, Cohen Z, Olivier A, Stanimirovic DB, Hamel E (1999). Functional acetylcholine muscarinic receptor subtypes in human brain microcirculation: identification and cellular localization. *J Cereb Blood Flow Metab* **19:** 794–802.

Ertl P, Rohde B, Selzer P (2000). Fast calculation of molecular polar surface area as a sum of fragment- based contributions and its application to the prediction of drug transport properties. *J Med Chem* **43:** 3714–3717.

Eshleman AJ, Carmolli M, Cumbay M, Martens CR, Neve KA, Janowsky A (1999). Characteristics of drug interactions with recombinant biogenic amine transporters expressed in the same cell type. *J Pharmacol Exp Ther* **289:** 877–885.

Gan X, Zhang L, Metz C, Bucala R, Newton T, Fiala M (1998a). IV cocaine administration modulates concomitantly the serum cortisol and its counter-regulatory hormones. *FASEB J* **12:** A186.

Gan X, Zhang L, Newton T, Chang S, Ling W, Kermani V, Berger O, Graves M, Fiala M (1998b). Cocaine infusion increases interferon-gamma and decreases interleukin-10 in cocaine-dependent subjects. *Clin Immunol Immunopathol* **89:** 181–190.

Gan X, Zhang L, Taub D, Chang S, Stins M, Kim K, Way D, Weinand M, Witte M, Graves M, Fiala M (1999). Cocaine enhances endothelial adhesion molecules and leukocyte migration. *Clin Immunol* **91:** 68–76.

Garcia JG, Schaphorst KL, Verin AD, Vepa S, Patterson CE, Natarajan V (2000). Diperoxovanadate alters endothelial cell focal contacts and barrier function: role of tyrosine phosphorylation. *J Appl Physiol* **89:** 2333–2343.

Glass JD, Fedor H, Wesselingh SL, McArthur JC (1995). Immunocytochemical quantitation of human immunodeficiency virus in the brain: correlations with dementia. *Ann Neurol* **38:** 755–762.

Goodkin K, Shapshak P, Metchs L, CB M, KA C (1998). Cocaine abuse and HIV-1 infection: Epidemiology and neuropathogenesis. *J Neuroimmunol* **83:** 88–101.

Gujuluva C, Burns AR, Pushkarsky T, Popik W, Berger O, Bukrinsky M, Graves MC, Fiala M (2001). HIV-1 penetrates coronary artery endothelial cells by transcytosis. *Mol Med* **7:** 169–176.

Holman BL, Garada B, Johnson KA, Mendelson J, Hallgring E, Teoh SK, Worth J, Navia B (1992). A comparison of brain perfusion SPECT in cocaine abuse and AIDS dementia complex. *J Nucl Med* 33: 1312–1315.

Kokkinos J, Levine SL (1993). Cocaine-associated cerebral vasculitis. *Neurol Clin* **11:** 577–591.

Koutsilieri E, Gotz ME, Sopper S, Sauer U, Demuth M, ter Meulen V, Riederer P (1997). Regulation of glutathione and cell toxicity following exposure to neurotropic substances and human immunodeficiency virus-1 in vitro. *J NeuroVirol* **3:** 342–349.

Liu NQ, Lossinsky AS, Popik W, Li X, Gujuluva C, Kriederman B, Roberts J, Pushkarsky T, Bukrinsky M, Witte M, Weinand M, Fiala M (2002). Human immunodeficiency virus type 1 enters brain microvascular endothelia by macropinocytosis dependent on lipid rafts and the mitogen-activated protein kinase signaling pathway. *J Virol* **76:** 6689–6700.

Lossinsky AS, Shivers RR (2003). *Studies of cerebral endothelium by scanning and high-voltage electron microscopy.* Humana Press: Totowa, NJ.

Nath A, Hauser KF, Wojna V, Booze RM, Maragos W, Prendergast M, Cass W, Turchan JT (2002). Molecular basis for interactions of HIV and drugs of abuse. *J Acquir Immune Defic Syndr* **31** (Suppl 2): S62–S69.

Nath A, Maragos WF, Avison MJ, Schmitt FA, Berger JR (2001). Acceleration of HIV dementia with methamphetamine and cocaine. *J NeuroVirol* 7: 66–71.

Price RW, Brew BJ (1988). The AIDS dementia complex. *J Infect Dis* **158:** 1079–1083.

Resnick L, Berger JR, Shapshak P, Tourtellotte WW (1988). Early penetration of the blood-brain-barrier by HIV. *Neurology* **38:** 9–14.

Sharma DP, Anderson M, Zink MC, Adams RJ, Donnenberg AD, Clements JE, Narayan O (1992). Pathogenesis of acute infection in rhesus macaques with a lymphocyte-tropic strain of simian immunodeficiency virus. *J Infect Dis* **166:** 738–746.

Stins MF, Prasadarao NV, Zhou J, Arditi M, Kim KS (1997). Bovine brain microvascular endothelial cells transfected with SV40- large T antigen: development of an immortalized cell line to study pathophysiology of CNS disease. *In Vitro Cell Dev Biol Anim* **33:** 243–247.

Wakayama K, Ohtsuki S, Takanaga H, Hosoya K, Terasaki T (2002). Localization of norepinephrine and serotonin transporter in mouse brain capillary endothelial cells. *Neurosci Res* **44:** 173–180.

Wiley CA, Achim CL, Christopherson C, Kidane Y, Kwok S, Masliah E, Mellors J, Radhakrishnan L, Wang G, Soontornniyomkij V (1999). HIV mediates a productive infection of the brain. *AIDS* **13:** 2055–2059.

Williams KC, Hickey WF (2002). Central nervous system damage, monocytes and macrophages, and neurological disorders in AIDS. *Annu Rev Neurosci* **25:** 537–562.

Zhang L, Looney D, Taub D, Chang SL, Way D, Witte MH, Graves MC, Fiala M (1998). Cocaine opens the blood-brain barrier to HIV-1 invasion. *J NeuroVirol* **4:** 619–626.